Text S1: Information on Kibale National Park and the Kanyawara Chimpanzee Community

Struhsaker [1] provides an overview of Kibale National Park, including forest ecology. The Kanywara chimpanzee community, which occupies roughly 40 km^2 of Kibale National Park [2], was partially habituated to human presence by M. Ghiglieri during 1979-1980 and G. Isabirye-Basuta during 1983-1985. The Kanyawara community was fully habituated to human observers by 1990 [3]. R. Wrangham founded the Kibale Chimpanzee Project (KCP) in 1987, and along with colleagues, has continuously collected data on chimpanzee life history, behavioral development, and social relationships (among other topics). Funding for KCP is provided by the U.S. National Science Foundation (awards 9807448 and 0416125), the U.S. National Institutes of Health, National Geographic Society, L.S.B. Leakey Foundation, and the Wenner-Gren Foundation.

To collect behavioral data for this paper, J. Rushmore worked alongside KCP researchers and field assistants. At the time of this study, the community was comprised of 48 chimpanzees with 12 adult males (aged > 14), 14 adult females (aged > 13), 9 immature males and 6 immature females (aged between 5-14 and 5-13 respectively; referred to throughout the main text as juveniles), and 7 dependent offspring (aged ≤ 4).

Text S2: Additional Methods

Basic reproductive number ($\overline{R_0}$)

Our $\overline{R_0}$ calculations strictly correspond to the basic reproductive rate definition typically used in epidemiology literature, where R_0 is the average number of secondary infections caused by one primary infection in a completely naïve population [4]. This R_0 definition (referred to here as PR_0 for primary infection R_0) has been used to model pathogen transmission on contact networks [5, 6]. However, several other studies use an alternate definition for R_0 in reference to network epidemiology, in which R_0 is the number of secondary infections caused by a randomly selected infected node [i.e., not the index case: 7, 8]. We will henceforth refer to this second definition as SR_0 (for secondary infection R_0).

PR_0 depends only on mean degree of the population and edge-specific transmissibilities (T_{ij}) of the pathogen, whereas SR_0 also depends on the variance of the degree distribution and clustering. Hence, using the basis of the PR_0 definition (which was then averaged across months to create $\overline{R_0}$ as described above) allowed us to assess the impact of network structure (month) on outbreak size for a pathogen characterized by a particular $\overline{R_0}$, without the circular issue of $\overline{R_0}$ also depending on inherent aspects of network structure (*e.g.,* degree distribution and clustering). Furthermore, using the definition of PR_0 allowed us to easily calculate $\overline{R_0}$ for a given $\beta\tau$, by averaging the expected number of secondary cases for each of the possible 37 index cases across the nine monthly networks. Using the definition of SR_0 to calculate $\overline{R_0}$ would require substantially more complicated simulations (i.e., calculating the expected number of secondary cases that result from a randomly selected secondary case for each of the 37 index cases across all nine months). Also, SR_0 may not be appropriate for simulating pathogen transmission on small networks, as basic reproductive rate estimates based on the number of secondary cases could be biased due to the network already being saturated. Lastly, we note that because PR_0 refers to the reproductive rate for an index case, which on average will have a lower mean degree than a secondary case, our $\overline{R_0}$ calculations are expected to be slightly lower than SR_0 calculations.

Permutation tests

The permutation-based regression test [9] uses node-level parameters (where each row in the dataset represents a node and columns provide attribute data for each node). The test first calculates the regression slope coefficients of the observed dataset; then, over 30,000 permutations, the algorithm randomly shuffles values of the dependent variable while leaving the values of the independent variables in place. Regression coefficients are recalculated after each permutation, and the P-value for each parameter is calculated by determining the proportion of permutations that yielded numbers with larger absolute values than the original regression for the observed dataset. This test controls for the interdependencies of network nodes. Because we observed a non-linear relationship between mean outbreak size and $\overline{R_0}$, we ran a separate model for each of the four $\overline{R_0}$ values.

Table S1: Chimpanzee trait data for study subjects (*n* = 37). This table shows the sex, age class, family size, and trait-based group for all chimpanzees included in the study.

chimpanzee ID	sex[1]	age class[2]	family size	trait-based group[3]
AJ	M	A	1	HM
AL	F	A	3	CR-L
AT	M	J	3	CR-L
AZ	M	J	3	CR-L
BB	M	A	1	HM
BL	F	A	3	ER
BO	M	J	3	ER
BU	F	J	3	ER
ES	M	A	2[4]	MM
EU	F	J	2[4]	CR-S
KK	M	A	1	HM
LK	M	A	1	HM
LR	F	A	1	CR-S
ML	F	A	1	ER
MS	M	A	1	HM
MU	F	A	2	ER
MX	M	J	2	ER
NP	F	J	1	CR-S
OG	M	J	4	CR-L
OM	F	J	4	CR-L
OT	F	J	4	CR-L
OU	F	A	4	CR-L
PB	M	A	1	LM
PG	M	A	1	MM
QT	F	A	1	CR-S
RD	F	A	1	ER
ST	M	A	1	MM
TG	F	A	4	CR-L
TJ	M	A	4	LM
TS	F	J	4	CR-L
TT	M	J	4	CR-L
TU	M	A	1	MM
UM	F	A	2	ER
UN	M	J	2	ER
WA	F	A	1	ER
WL	F	A	1	CR-S
YB	M	A	1	LM

[1]Sex: M=male, F=female
[2]Age Class: A=adult, J=juvenile [as defined in ref. 10]
[3]Trait-based group: HM, MM, and LM refer to high-, medium-, and low-ranking adult males, respectively; CR-L refers to core-ranging adult females and juveniles with families larger than 2 members; CR-S refers to core-ranging adult females and juveniles with families smaller than 3 members; ER refers to edge-ranging adult females and juveniles
[4]Even though their mother was deceased, ES and EU (a brother-sister pair) were considered a family unit, as ES and EU spent more than 65% of their time together

Table S2: Comparison of minimum coverage requirements across vaccination strategies

a. Minimum Coverage Threshold:

vaccination strategy	$\overline{R_0} = 0.7$	$\overline{R_0} = 1.5$	$\overline{R_0} = 3.0$	$\overline{R_0} = 10.0$
centrality-based	0% (0)	2.70% (1)	18.92% (7)	32.43% (12)
trait-based	0% (0)	2.70% (1)	21.62% (8)*	32.43% (12)
random	0% (0)	5.41% (2)	24.32% (9)	37.84% (14)

b. Conservative Coverage Threshold:

vaccination strategy	$\overline{R_0} = 0.7$	$\overline{R_0} = 1.5$	$\overline{R_0} = 3.0$	$\overline{R_0} = 10.0$
centrality-based	0% (0)	27.03% (10)	45.95% (17)	62.16% (23)
trait-based	5.41% (2)	35.14% (13)*	45.95% (17)	64.86% (24)
random	8.11% (3)	43.24% (16)	56.76% (21)	67.57% (25)

For each vaccination strategy, the coverage threshold is provided as a percentage of the community, with the number of individuals vaccinated in parentheses, for A) the mean outbreak size to affect < 30% of the community (Minimum Coverage Threshold), and B) an outbreak to affect < 30% of the community in at least 95% of the simulations (Conservative Coverage Threshold). The table shows results for trait-based simulations using a single adult male category (M). Results were identical for simulations using this category M or three adult male categories (HM, MM, LM; see Results), except for a couple instances (*) in which simulations using HM, MM, and LM categories required vaccinating one less individual.

Figure S1. Comparing bond percolation and temporal chain-binomial model outcomes for pathogen transmission in proximity networks

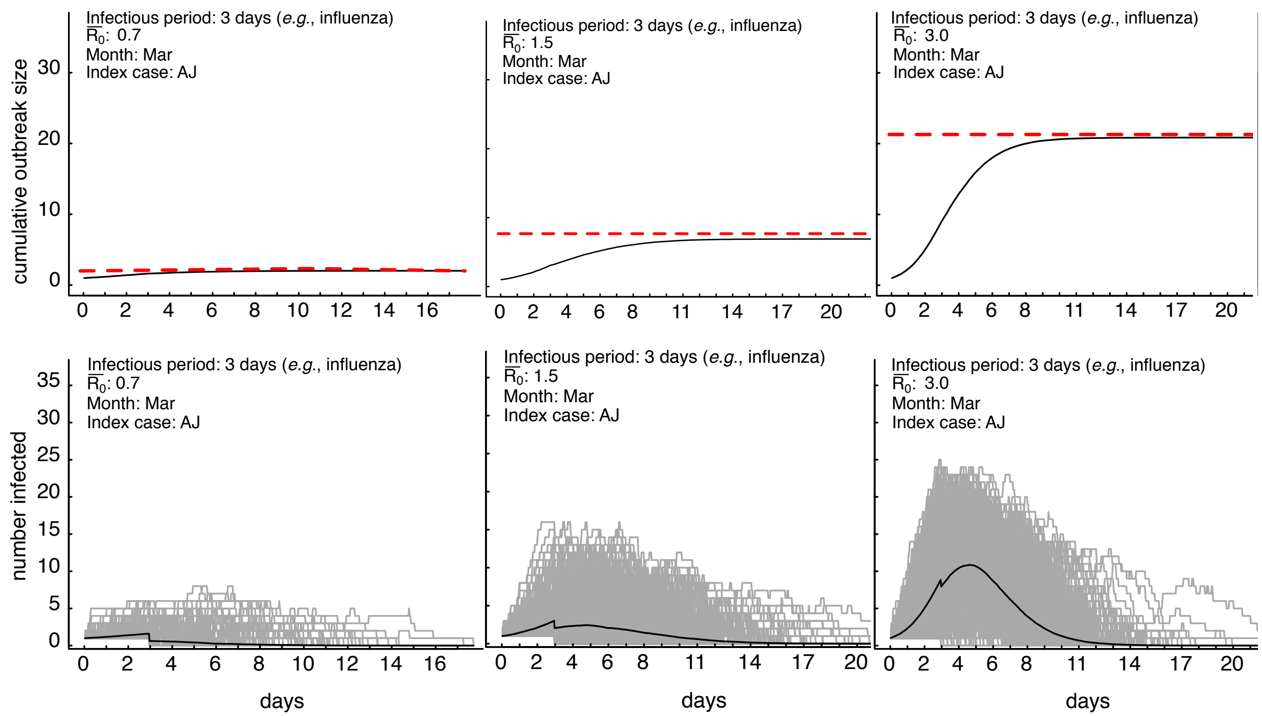

The top row shows cumulative outbreak size over time for a range of $\overline{R_0}$ values (by panel) using a temporal chain binomial model with a fixed recovery rate (solid black line) and the mean final outbreak size as determined by bond percolation (dotted red line). These panels confirm that chain binomial and bond percolation model outcomes were consistent. The bottom row shows 1000 simulations (grey lines) of the number of infected individuals over time for a range of $\overline{R_0}$ values (by panel) using a temporal chain binomial model. The solid black line shows the average number of individuals infected over time (*i.e.*, averaged across the 1000 simulations).

Figure S2. Relationship between monthly network density and mean outbreak size

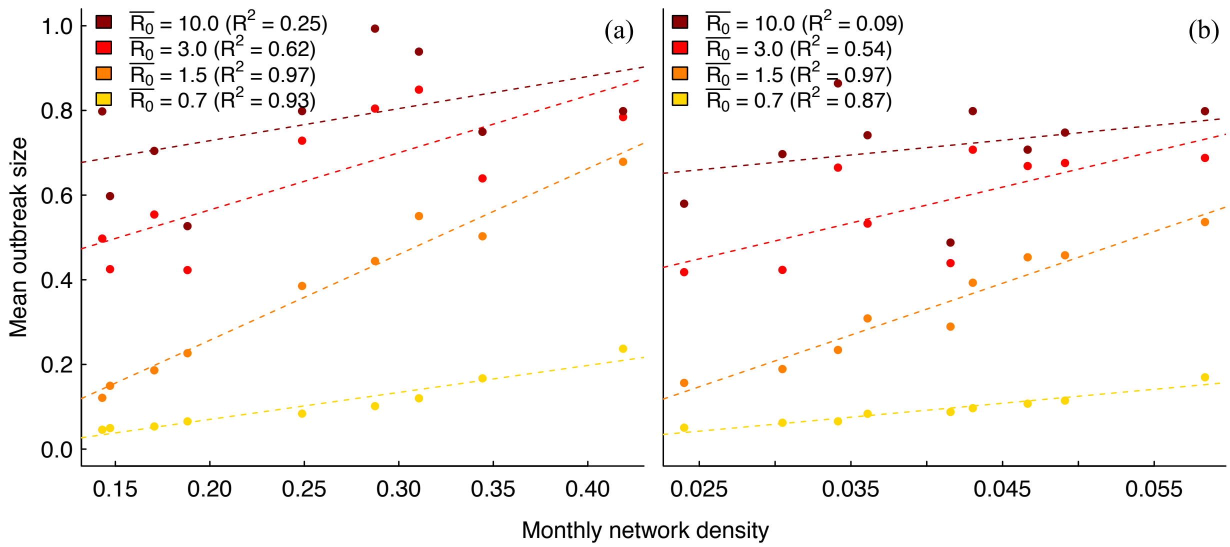

Coefficients of determination are shown between monthly network density and mean outbreak size (averaged across all index cases) for four different $\overline{R_0}$ values for party networks (a) and proximity networks (b). Note that for lower $\overline{R_0}$ values, when density is low the pathogen only reaches a small proportion of the community leading to small outbreak sizes; when density is high, outbreaks can spread to more individuals and lead to relatively large mean outbreak sizes. Alternatively, for higher $\overline{R_0}$ values (particularly when $\overline{R_0}$ reaches 10), the pathogen can quickly spread to a large proportion of the population regardless of network density. Thus, our simulations showed that network density plays a more important role in determining mean outbreak size when pathogens have a low to moderate level of infectiousness than when pathogens are highly contagious.

Figure S3. Evaluation of vaccination strategies on party networks by the Conservative Coverage Threshold

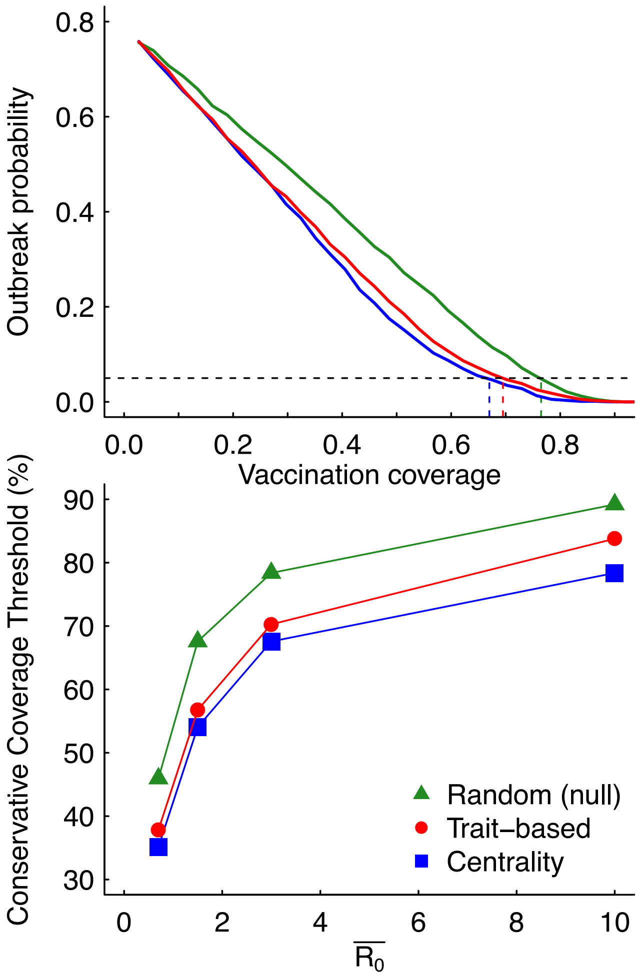

The top panel shows the outbreak probability (the proportion of simulations resulting in an outbreak greater than 10% of the community) for centrality-based vaccinations (blue), trait-based vaccinations (red), and random vaccinations (green) at varying levels of coverage (shown as a proportion of the community) when $\overline{R_0} = 3.0$. The black dotted line marks the Conservative Coverage Threshold, at which no more than 5% of the simulations result in outbreaks. The bottom panel shows this Conservative Coverage Threshold for each vaccination strategy and $\overline{R_0}$ combination.

Figure S4. Mean outbreak size results for pathogen transmission simulations on party-level chimpanzee networks

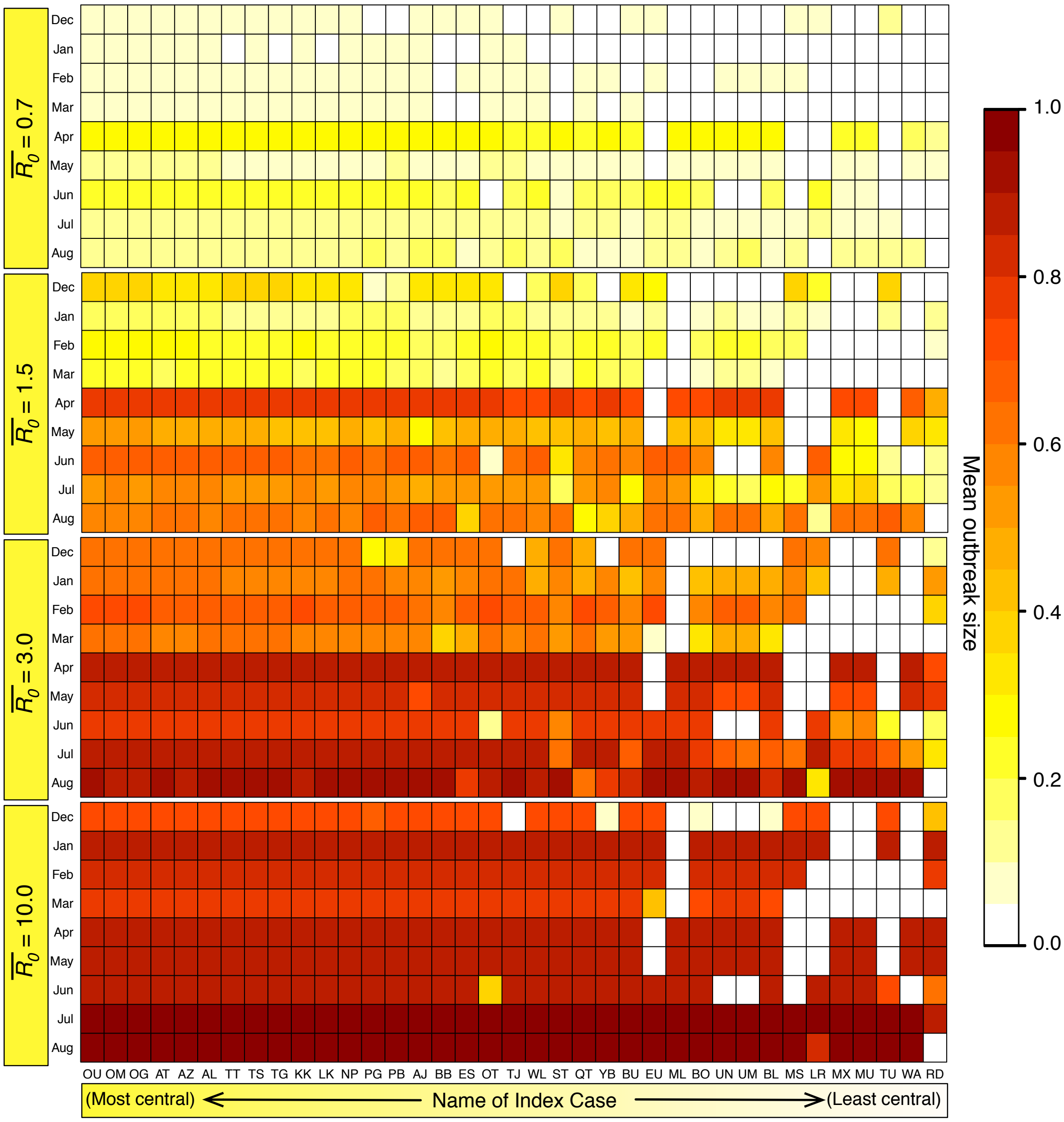

The color of each cell shows the average proportion of the community (n = 37) that was infected across the 1000 replicates per unique combination of parameters The x-axis shows the identities of the index cases, ordered from highest to lowest mean weighted degree centrality (i.e., averaged across months). Estrous females were present during Jan (n = 1 estrous female), Apr (n = 1), May (n = 1), Jun (n = 1), Jul (n = 2), and Aug (n = 2).

References:

1. Struhsaker, T.T. 1997 *Ecology of an African rain forest: logging in Kibale and the conflict between conservation and exploitation*. Gainesville: University Press of Florida.
2. Wilson, M.L., Kahlenberg S.M., Wells M., Wrangham R.W. 2012 Ecological and social factors affect the occurrence and outcomes of intergroup encounters in chimpanzees. *Anim Behav* **83**(1), 277-291.
3. Wrangham, R.W., Clark A.P., Isabirye-Basuta G. 1992 Female social relationships and social organization of Kibale Forest chimpanzees. In *Topics in primatology* (eds. Nishida, T., McGrew W.C., Marler P., Pickford M., de Waal F.B.M.), pp. 81-98. Tokyo, Univesity of Tokyo Press.
4. Anderson, R.M., Medley G., May R., Johnson A. 1986 A preliminary study of the transmission dynamics of the human immunodeficiency virus (HIV), the causative agent of AIDS. *Math Med Biol* **3**(4), 229-263.
5. Hamede, R., Bashford J., Jones M., McCallum H. 2011 Simulating devil facial tumour disease outbreaks across empirically derived contact networks. *J Appl Ecol*.
6. Davis, S., Trapman P., Leirs H., Begon M., Heesterbeek J. 2008 The abundance threshold for plague as a critical percolation phenomenon. *Nature* **454**(7204), 634-637.
7. Meyers, L.A. 2007 Contact network epidemiology: Bond percolation applied to infectious disease prediction and control. *Bull Am Math Soc* **44**(1), 63.
8. Newman, M.E.J. 2002 Spread of epidemic disease on networks. *Phys Rev E* **66**(1), 016128.
9. Hanneman, R.A., Riddle M. 2005 Introduction to social network methods. (Riverside, CA, University of California Riverside.
10. Rushmore, J., Caillaud D., Matamba L., Stumpf R.M., Borgatti S.P., Altizer S. *2013* Social network analysis of wild chimpanzees provides insights for predicting infectious disease risk. *J Anim Ecol* **82**, 976–986. (doi:10.1111/1365-2656.12088).